

INNOVATIVE TECHNOLOGIES OF OIL AND GAS

APPLICATION OF MULTI-VERTICAL WELL SYNCHRONOUS HYDRAULIC FRACTURING TECHNOLOGY FOR DEEP COALBED METHANE (DCBM) PRODUCTION

Zhaozhong Yang,¹ Rui He,¹ Xiaogang Li,¹ Zhanling Li,²
Ziyuan Liu,³ and Yanjun Lu⁴

In this paper, we propose a method for multi-vertical well synchronous hydraulic fracturing and compare with synchronous fracturing technologies used in shale. Based on theoretical analysis and triaxial fracturing experiments, we have shown that “face interference” in multi-vertical well synchronous fracturing helps to connect the cleats and generate complex fracture networks. The developed three-step method for designing synchronous fracturing technology was tested under field conditions. The results showed that application of synchronous fracturing decreases the gas breakthrough time in the wells and increases DCBM (deep coalbed methane) production. Furthermore, stress interference generated by synchronous fracturing has a positive impact on the production rate of wells adjacent to the experimental area.

Keywords: *deep coalbed methane (DCBM), synchronous hydraulic fracturing, stress interference, design method.*

Proved coalbed methane (CBM) reserves are found in more than seventy countries.

¹State Key Laboratory of Oil and Gas Reservoir Geology and Exploitation, Southwest Petroleum University, Chengdu, China. ²China Nuclear Engineering & Construction Group Corporation Limited, Beijing, China. ³Sichuan Energy Investment Group Co., Ltd., Chengdu, China. ⁴Moscow Lomonosov State University, Moscow, Russia. *E-mail: yangzhaozhongswpu@163.com.* Translated from *Khimiya i Tekhnologiya Topliv i Masel*, No. 3, pp. 57 – 63, May – June, 2019.

According to geological survey data, China is ranked third in the world in coalbed methane reserves at a depth lower than 2000 m, volume 36.81 trillion m³ [1]. The Chinese government supports investment in exploiting CBM. The volume of methane reserves at a depth lower than 1000 m is 62.2% of the proved reserves. In recent years, attention has increasingly been focused on exploiting DCBM in China [2].

Geological survey data show that DCBM reservoirs are characterized by the following parameters:

- The geological structure of the reservoirs is characterized by the presence of a stress field. The cleats are more widely distributed in deep coalbeds.
- Under high temperature and high stress conditions, the coal reservoir permeability and its mechanical properties are nonuniformly distributed.
- The reservoir exhibits significant heterogeneity in properties in the horizontal and vertical directions, and high values of the principal stress and stress difference in the horizontal direction.

Hydraulic fracturing is widely used in exploiting CBM reserves [3, 4]. The following difficulties arise in application of DCBM fracturing.

1. The low porosity and permeability of deep coalbeds makes flow of methane in a porous medium difficult [5]. As a result, the fracturing technology applicable in shallow coalbeds is not effective in deep coalbeds.
2. Deep coalbeds have a quite well developed natural fracture system [6], including face cleats and butt cleats. Generally active water with low viscosity is used as the fracturing fluid. Then the filtration losses increase, and the likelihood of forming a long fracture is reduced.
3. Because of the large fracturing fluid losses [7], the proppant is difficult to be transported by the active water.

For DCBM reservoirs, characterized by a high horizontal principal stress difference, the conventional single-well fracturing technology does not generate a large number of cleats. As a result, the stimulated reservoir volume (SRV) is small [8]. In this case, the gas drainage area and the volume of methane production are not large. We need to propose a new technology for exploiting DCBM which will let us activate and connect the cleats and increase the SRV [9].

Published data on the Fort Worth Basin (Texas USA) show that application of synchronous fracturing in two adjacent horizontal shale gas wells resulted in a significant increase in production [10-12]. Analysis of the data showed that the increase in shale gas production is explained by superposition (interference) of stresses generated by fracturing in the adjacent well [13]. Earlier research indicated that the generated hydraulic fracture induces stress in the surrounding area. Applying the displacement discontinuity method (DDM), for each element i we can calculate the induced stress using the formula [14]:

$$\sigma_s^i = \sum_{j=1}^N A_{ss}^{i,j} D_s^j + \sum_{j=1}^N A_{sn}^{i,j} D_n^j \quad (1)$$

$$\sigma_n^i = \sum_{j=1}^N A_{ns}^{i,j} D_s^j + \sum_{j=1}^N A_{nn}^{i,j} D_n^j$$

where σ_s^i is the shear stress for the midpoint of element i , MPa; σ_n^i is the normal stress for the midpoint of

element i , MPa; $A_{ss}^{i,j}$, $A_{sn}^{i,j}$, $A_{ns}^{i,j}$, $A_{nn}^{i,j}$ are the boundary stress influencing factors, MPa/m; D_s^j is the tangential displacement discontinuity of element j , m; D_n^j is the normal displacement discontinuity of element j , m.

The final horizontal stress can be expressed as:

$$\sigma'_H = \sigma_H + \sigma_{inH} \quad (2)$$

$$\sigma'_h = \sigma_h + \sigma_{inh}$$

where σ'_H , σ'_h are respectively the final maximum and minimum horizontal principal stress, MPa; σ_H , σ_h are respectively the initial maximum and minimum horizontal principal stress, MPa; σ_{inH} , σ_{inh} are respectively the induced stress in the direction of the maximum horizontal principal stress and the induced stress in the direction of the minimum horizontal principal stress, MPa.

Typically the induced stress in the direction of the horizontal minimum principal stress is significantly higher than the induced stress in the direction of the maximum horizontal principal stress (Fig. 1). Thus in the stress interference area, the minimum horizontal principal stress increases much more than the maximum horizontal principal stress, and consequently the horizontal stress difference decreases even to reorientation of the horizontal principal stress direction. Under such conditions, coal cleats are easily opened and connected, forming a fracture network. Assessing the positive results of synchronous fracturing for shale gas, we proposed a multi-vertical well synchronous fracturing technology for DCBM. The technology has the following advantages.

1) In a deep coalbed, face cleats and butt cleats are formed that are more widely distributed than natural fractures in shale. The cleats are connected during synchronous fracturing.

2) With synchronous fracturing of horizontal wells, the fracturing operation is carried out in stages from the well toe to the well heel. In each stage, two fractures are formed simultaneously that are directed along the same line, and the interference area is mainly distributed in the region between the fracture tips (“tip interference”) (Fig. 2a). For vertical wells, the stress interference area is widely distributed between the two parallel fractures (“face interference”) (Fig. 2b). Obviously such “face interference” has an advantage over “tip

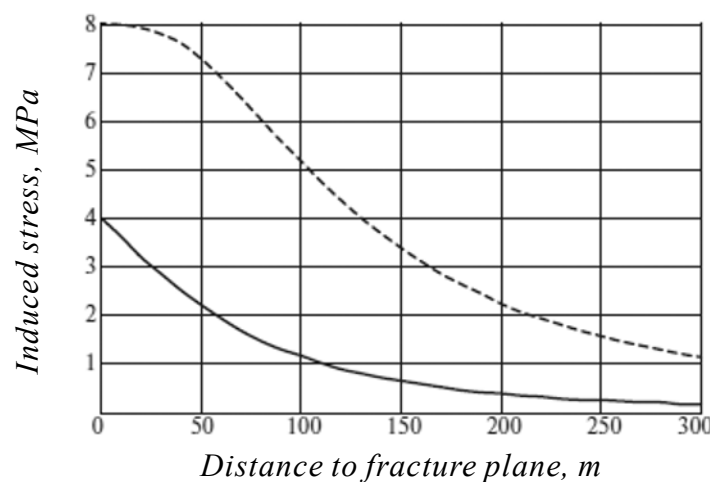


Fig. 1 Induced stress in the direction of minimum (dashed line) and maximum (solid line) horizontal principal stress.

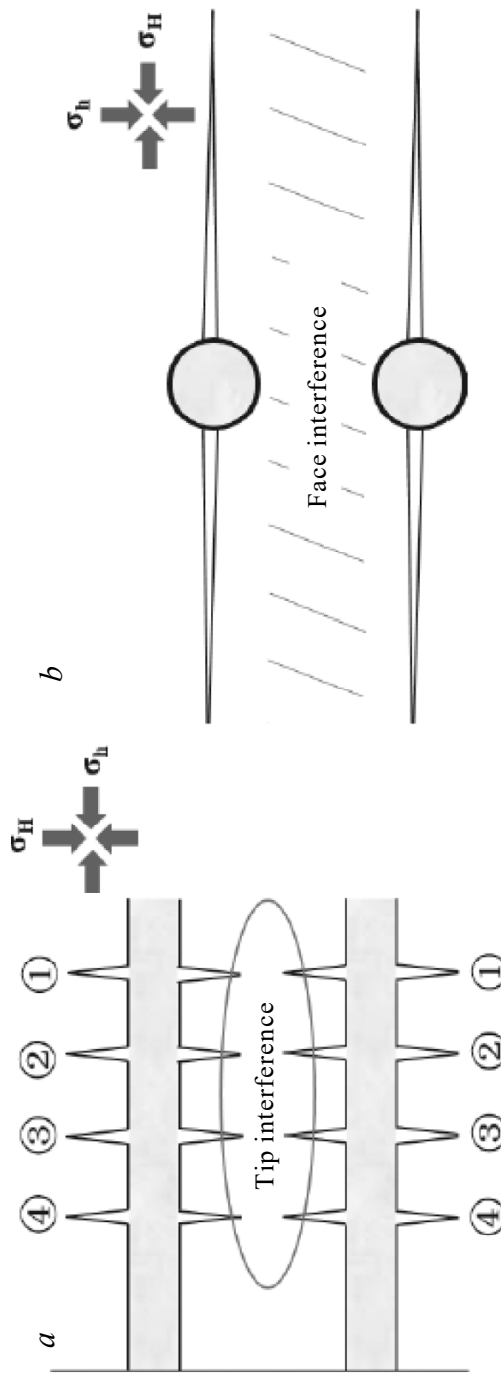


Fig. 2 Synchronous fracturing when using two horizontal (a) and two vertical (b) wells.

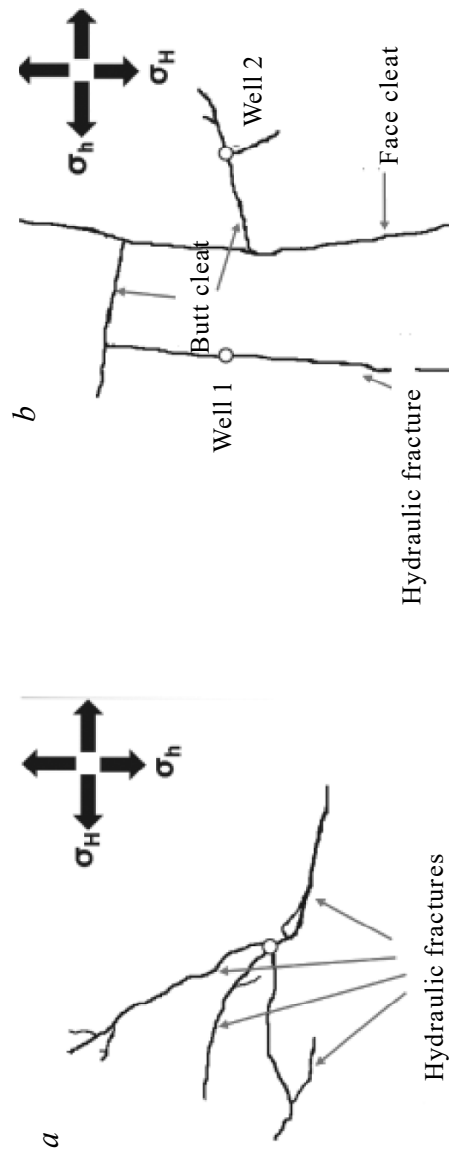


Fig. 3 Sketch of experimental results for single-well (a) and synchronous (b) fracturing.

interference” and generates a fracture network. Theoretically, the more vertical wells participating in the synchronous fracturing operation, the more effective the stress interference becomes.

3. In contrast to shale gas, when exploiting CBM the water drainage period is much longer, even as long as several years [15]. We can significantly shorten the water drainage time by using synchronous fracturing, in which the coalbed is broken into many blocks and high pressure drop areas appear in the reservoir. When using more than two wells, a wider pressure drop area is formed, synchronous water drainage effectively reduces the reservoir pressure, and the gas production volume significantly increases.

Triaxial simulation was used to experimentally study fracture propagation [16]. The experimental samples of high rank coal ($30 \times 30 \times 30$ cm cubic blocks) were obtained from samples drilled from a deep coalbed in Qinshui Basin (China). In order to simulate a vertical well, we used a steel tube of diameter 1 cm. The role of the fracturing fluid was played by active water, colored by a red dye. The face cleat was parallel to the direction of the maximum horizontal principal stress. In the experiments, we used two coal samples: one to simulate single-well fracturing, and the other to simulate synchronous fracturing. The experimental conditions were the following: vertical stress 14.2 MPa, maximum horizontal principal stress 15 MPa, and minimum horizontal principal stress 11.3 MPa.

The results showed that in simulating single-well fracturing, multiple fractures appear in the sample but

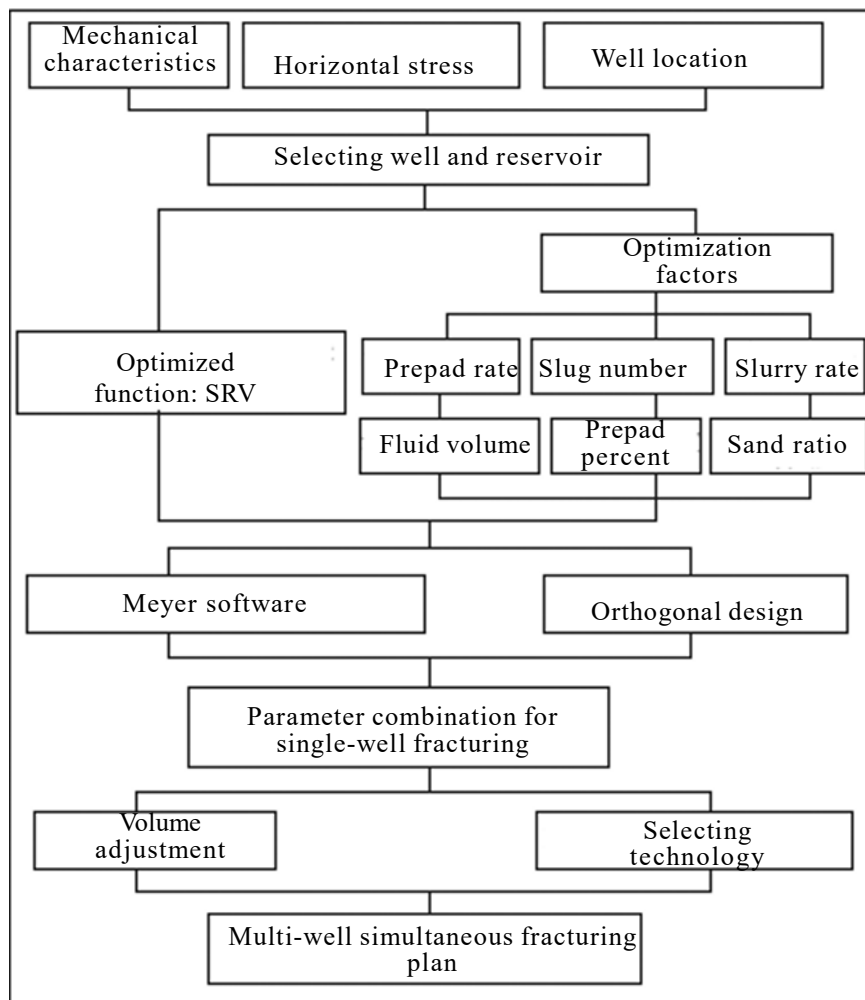


Fig. 4 Flow chart for designing synchronous multi-well vertical fracturing technology.

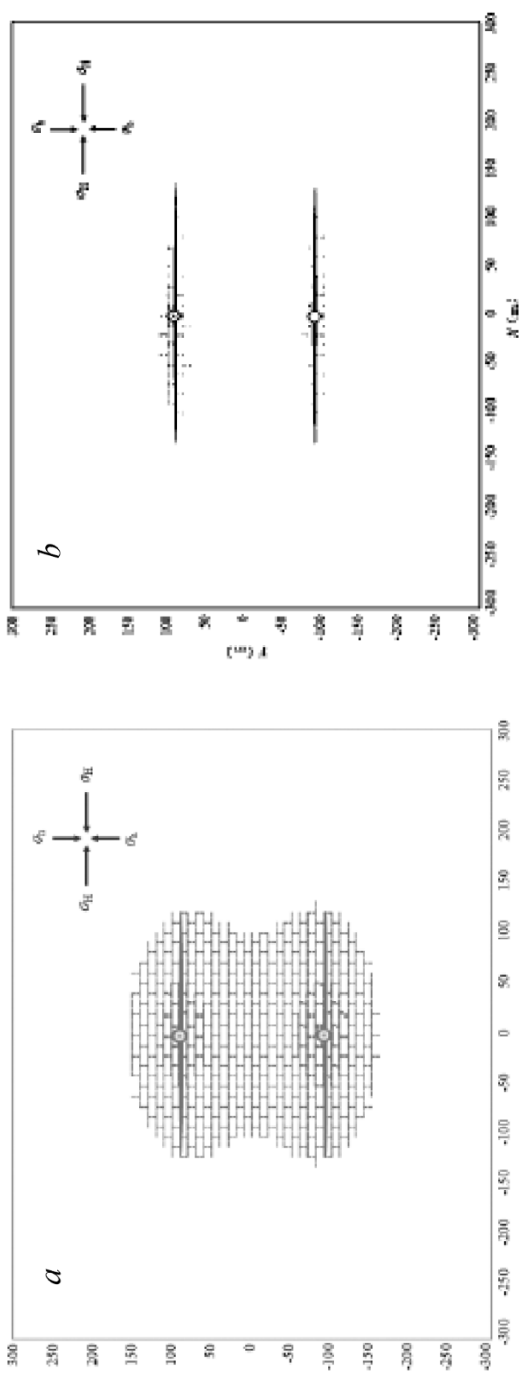


Fig. 5 Simulation of connected (a) and independent (b) fracture network.

they did not open the cleat, and no fracture network was formed (Fig. 3a). In the experiment with two synchronous wells (simultaneous fracturing), for the same load conditions the fracture pattern is quite different (Fig. 3b). First of all, a hydraulic fracture is initiated from well 1 along the line of maximum horizontal principal stress, from which a butt cleat is formed because of stress interference from well 2. With further propagation, it is connected with the face cleat between wells 1 and 2. On the other hand, the hydraulic fracture of well 2 propagates in the direction along the butt cleat and is connected with the line of the face cleat. In contrast to single-well fracturing, with synchronous fracturing the hydraulic fractures, face cleats, and butt cleats form a fracture network.

The design method for the multi-well synchronous fracturing operation includes three stages: selecting the wells and reservoirs, optimizing the fracturing parameters for each well, and optimizing the parameters for synchronization of the wells. Fig. 4 shows the flow chart for the design algorithm.

Propagation of the fracture network is simulated by the discrete element method (DEM) based on initial data for the mechanical properties of the coal matrix and cleats, the vertical stress values, and the fracturing parameters [17]. Selection of the optimal wells and reservoirs is based on comparing the calculated area of the fracture network for different input parameters. The simulation results for hydraulic fracturing show that a high initial value for the horizontal stress difference has an unfavorable impact on the effectiveness of forming the fracture network. When the horizontal principal stress difference is less than 6 MPa, the fracture networks created by each well can be satisfactorily connected (Fig. 5a). For coalbeds with a high Poisson's ratio, the fracture network for each well is not large. As shown in Fig. 5b, if Poisson's ratio is equal to 0.4, the regions of induced fractures do not intersect. Theoretically, the recommended value of Poisson's ratio should be less than 0.3. Furthermore, a complex fracture network is more effectively formed for longer fractures, higher fracture

Table 1

Factors	Fluid volume, m ³	Prepad fracturing fluid, %	Prepad rate, m ³ /min	Slurry rate, m ³ /min	Average sand ratio, %	Slug number
Level 1	450	25	4	6	9	0
Level 2	500	30	5	6.5	10	1
Level 3	550	35	6	7	11	2
Level 4	600	40	7	7.5	12	3
Level 5	650	45	8	8	13	4

Table 2

SRV, m ³					
fluid volume	prepad percentage	prepad rate	slurry rate	average sand ratio	slug number
31730	28790	37700	39110	39060	28940
35660	34190	41060	39660	38160	30780
38460	40750	38440	38220	39860	40230
47770	44040	41230	38130	39480	45040
42370	48220	37550	40870	37420	49100

net pressure, and lower fracturing fluid viscosity. The distance between wells and selection of the number of wells (more than two) also affect the appearance and expansion of the stress interference region and formation of the fracture network.

The parameters for each well are optimized with respect to the volume of the stimulated reservoir volume (SRV). Based on field data, we select the optimized parameters of the well: the fracturing fluid volume, the prepad fracturing fluid percentage and the prepad rate, the slurry rate, the average sand ratio, and the slug number. We used the Meyer software for the optimization (a popular program for simulating hydraulic fracturing). Optimization was done by constructing an orthogonal design $L_{25}(5^6)$, containing 6 parameters and 5 factor levels (Table 1). For optimization of the SRV, it is sufficient to carry out 25 simulation experiments for different parameter combinations. Table 2 shows the visual analysis of the results for the average SRV for each parameter, the maximum SRV for each parameter corresponds to the optimal parameter combination (level). We can see that the optimal parameter combination for single-well fracture is as follows: fluid volume 600 m^3 , prepad percentage 45%, prepad rate $7 \text{ m}^3/\text{min}$, average sand ratio 11%, slug number 4.

In order to enhance the stress interference effect in the synchronous fracturing technology, we selected four wells with parameters corresponding to the required conditions (Fig. 6). Target coalbed No. 3 belongs to a deep coalbed. In order to increase the SRV, the injected fracturing fluid in the two farthest wells (I and IV) was increased to 800 m^3 , which guarantees sufficient fracture length and helps expand the area of stress interference. The remaining two wells were injected with 600 m^3 of fracturing fluid. Furthermore, during the entire fracturing period, fracturing was accompanied by injection of proppant to increase the fracture net pressure and the SRV. The amount of proppant was selected so that the best fracture conductivity would be achieved.

The synchronous fracturing technology was successfully used in the four selected wells. The microseismic monitoring results [18] show that a fracture network was generated in all four wells (see Fig. 6), and the SRV for each well is 4.76×10^5 to $1.054 \times 10^6 \text{ m}^3$ (Table 3). On the other hand, we observed deviation of the fracture azimuths for each well from the maximum horizontal principal stress direction, which is quite consistent with the triaxial simulation results.

Table 4 shows the production data. We see that the four wells participating in the synchronous fracturing initially showed gas production within 62 days, i.e., much earlier than the adjacent conventional wells (such as VII, VIII, IX). The critical desorption pressure for the four wells ranged between 2.2 MPa and 3.5 MPa, which is relatively high. As a result, gas production is significantly easier with synchronous fracturing. The gas production volume in these wells is significantly higher: in three of them, the daily gas production was greater than $800 \text{ m}^3/\text{day}$ in January 2018 (Fig. 7). We also see that the casing pressure

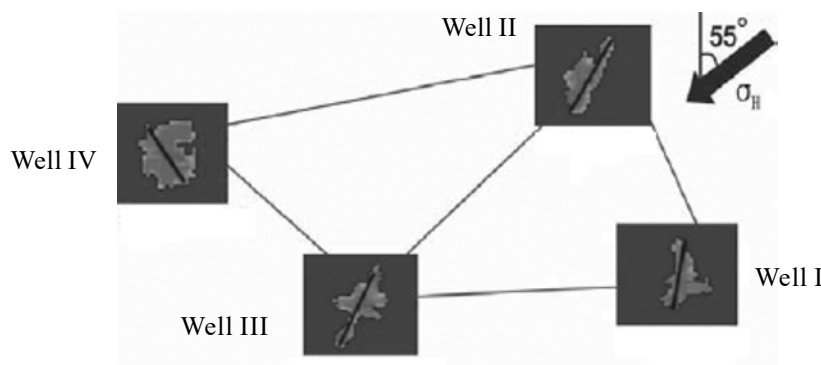


Fig. 6 Stimulated area from microseismic monitoring.

Table 3

Well	Main fracture length, m	Azimuth	Fracture network range, m		SRV, m ³
			from east to west	from north to south	
I	240	NE 9°	130	240	624000
II	260	NE 30°	140	220	616000
III	310	NE 25°	170	310	1054000
IV	180	NW 40°	140	170	476000

Table 4

Well type	Well number	Gas breakthrough time, days	Critical desorption pressure, MPa	Casing pressure, MPa	Average daily gas production in January 2018, m ³	Average daily water production in January 2018, m ³
Synchronous fracturing wells	I	15	2.8	0.16	956	0.1
	II	14	2.2	0.25	353	0.1
	III	8	3.5	0.38	802	0.1
	IV	62	2.9	0.30	1001	0.1
Adjacent wells experiencing interference from synchronous fracturing	V	14	2.3	0.77	413	0.1
	VI	14	2.7	0.30	518	0.1
Adjacent wells not experiencing interference from synchronous fracturing	VII	996	1.4	0	0	0
	VIII	no gas	—	0	0	0
	IX	265	1.6	0	0	0

in each well remains stable for DCBM production. Water production from each well remains at a low level and does not exceed 0.1 m³/day, which means good seepage channels for gas production.

In two adjacent wells (V and VI), single-well fracturing was implemented earlier. In order to increase gas production in these wells, they began to drain water at the same time as the four synchronous fracturing wells. The results showed that in wells V and VI, we also observed good production capacity. The gas breakthrough time for the two wells was no more than 14 days (see Table 4). Obviously the stress interference area induced by synchronous fracturing spreads to the two adjacent wells, and leads to a significant pressure drop, which helps gas desorption and an increase in production. In the other three adjacent wells (VII, VIII, and IX), no synchronous

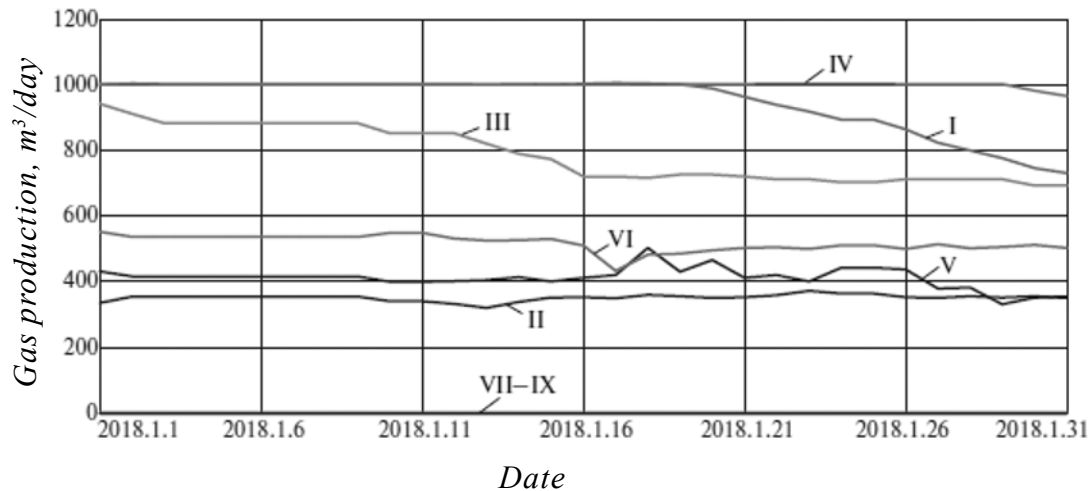


Fig. 7 Gas production for different wells (see numbers on curves).

fracturing was implemented and they did not drain water at the same time as the other wells. As a result, in these wells we did not observe a rapid drop in reservoir pressure, and the gas breakthrough time was significantly longer.

We can conclude that application of multi-vertical well synchronous fracturing technology helps increase production not only in the wells undergoing the fracturing operation, but also in adjacent wells. The developed technology can be successfully used to develop DCBM vertical wells.

This research was financially supported by the National Foundation for Major Projects in Science and Technology of China (2011ZX05042-002-001) and the Qihang Foundation of Southwest Petroleum University (No. 431).

REFERENCES

1. S. Li, D. Tang, Z. Pan et al., "Geological conditions of deep coalbed methane in the eastern margin of the Ordos Basin, China: Implications for coalbed methane development," *Journal of Natural Gas Science & Engineering*, 53 (2018).
2. Y. Lu, Z. Yang, X. Li et al., "Problems and methods for optimization of hydraulic fracturing of deep coal beds in China," *Chemistry & Technology of Fuels & Oils*, 51, No. 1, 41-48 (2015).
3. J. Zou, W. Chen, J. Yuan et al., "3-D numerical simulation of hydraulic fracturing in a CBM reservoir," *Journal of Natural Gas Science & Engineering*, 37 (2016).
4. Q. Feng, J. Liu, Z. Huang et al., "Study on the optimization of fracturing parameters and interpretation of CBM fractured wells," *Journal of Natural Gas Geoscience* (2018).
5. Y. Geng, D. Tang, H. Xu et al., "Experimental study on permeability stress sensitivity of reconstituted granular coal with different lithotypes," *Fuel*, 202, 12-22 (2017).
6. M. S. A. Perera, P. G. Ranjith, D. R. Viete et al., "Parameters influencing the flow performance of natural cleat systems in deep coal seams experiencing carbon dioxide injection and sequestration," *International Journal of Coal Geology*, 104, No. 1, 96-106 (2012).
7. J. X. Han, Z. Z. Yang, H. L. Wang et al., "Leak-off model of fracturing fluid in coal seam," *Journal of China Coal Society*, 39(S2), 441-446 (2014).

8. Y. Hu, Z. Li, J. Zhao et al., "Prediction and analysis of the stimulated reservoir volume for shale gas reservoirs based on rock failure mechanism," *Environmental Earth Sciences*, 76, No. 15, 546 (2017).
9. X. Weng, O. Kresse, C. E. Cohen et al., "Modeling of hydraulic fracture network propagation in a naturally fractured formation," *SPE Production & Operations*, 26, No. 4, 368-380 (2011).
10. W. Gary, G. W. Schein, and S. Weiss, "Simultaneous fracturing takes off: Enormous multiwell fracs maximize exposure to shale reservoirs, achieving more production sooner," *E & P*, 81, No. 3, 55-58 (2008).
11. G. A. Waters, B. K. Dean, R. C. Downie, K. J. Kerrihard, L. Austbo, and B. McPβherson, "Simultaneous hydraulic fracturing of adjacent horizontal wells in the Woodford shale," *SPE Hydraulic Fracturing Technology Conference, Woodlands, January 19-21, 2009*.
12. J. Yao, Q. D. Zeng, Z. Q. Huang et al., "Numerical modeling of simultaneous hydraulic fracturing in the mode of multi-well pads," *Science China Technological Sciences*, 60, No. 2, 232-242 (2017).
13. B. Sobhaniaragh, W. J. Mansur, and F. C. Peters, "The role of stress interference in hydraulic fracturing of horizontal wells," *International Journal of Rock Mechanics & Mining Sciences*, 106, 153-1 (2018).
14. X. G. Li, L. P. Yi, and Z. Z. Yang, "Numerical model and investigation of simultaneous multiple fracture propagation within a stage in horizontal well," *Environmental Earth Sciences*, 76, No. 7, 273 (2017).
15. D. Gao, Y. Liu, Z. Guo et al., "A study on optimization of CBM water drainage by well-test deconvolution in the early development stage," *Water*, 10, No. 7, 929.64 (2018).
16. T. Fan, G. Zhang, and J. Cui, "The impact of cleats on hydraulic fracture initiation and propagation in coal seams," *Petroleum Science*, 11, No. 4, 532-539 (2014).
17. W. Chen, H. Konietzky, C. Liu et al., "Hydraulic fracturing simulation for heterogeneous granite by discrete element method," *Computers & Geotechnics*, 95, 1-15 (2018).
18. G. Rodriguez-Pradilla, "Microseismic monitoring of a hydraulic-fracturing operation in a CBM reservoir: Case study in the Cerrejón Formation, Cesar-Ranchería Basin, Colombia," *Geophysics: The Leading Edge of Exploration*, 34, No. 8, 896-902 (2015).